4.5-/4.9-GHz-Band Selective High-Efficiency GaN HEMT Power Amplifier by Characteristic Impedance Switching

doi: 10.1587/transele.E101.C.751

PAPER Special Section on Microwave and Millimeter-Wave Technologies

4.5-/4.9-GHz-Band Selective High-Efficiency GaN HEMT Power Amplifier by Characteristic Impedance Switching

Kazuki MASHIMO[†a)], **Ryo ISHIKAWA**[†b)], ***Members***, ***and*** **Kazuhiko HONJO**[†c)], ***Fellow***

SUMMARY A 4.5-/4.9-GHz band-selective GaN HEMT high-efficiency power amplifier has been designed and evaluated for next-generation wireless communication systems. An optimum termination impedance for each high-efficiency operation band was changed by using PIN diodes inserted into a harmonic treatment circuit at the output side. In order to minimize the influence of the insertion loss of the PIN diodes, an additional line is arranged in parallel with the open-ended stub used for second harmonic treatment, and the line and stub are connected with the PIN diodes to change the effective characteristic impedance. The fabricated GaN HEMT amplifier achieved a maximum power-added efficiency of 57% and 66% and a maximum drain efficiency of 62% and 70% at 4.6 and 5.0 GHz, respectively, with a saturated output power of 38 dBm, for each switched condition.

key words: *power amplifier, high efficiency, band selective, GaN HEMT, PIN diode*

1. Introduction

In order to increase the capacity and data rate in mobile wireless communication systems, frequency-selective multi-band operations at an increased frequency range above 4 GHz are required for transmitter power amplifiers. Since the power amplifier consumes a large part of the supplied DC power to a transmitter, high-efficiency design approaches, such as class-E [1], class-F [2], class-J [3], and reactive harmonic termination-type (class-R) [4]–[8] amplifiers, are mandatory. However, these high-efficiency designs require optimized load impedances not only for the fundamental frequency but also for multi-harmonic frequencies.

In class-E amplifiers, frequency-selective design is performed by changing the parallel capacitance at the output current source so that the power factor for the fundamental frequency is optimized [9], [10]. However, this optimization usually breaks the condition of harmonic frequency optimizations. The class-F design approach allows for a very narrow load impedance design space, where loads for even harmonic frequencies should be short-circuited and those for odd harmonic frequencies should be open [11]. The approach for class-J amplifiers brings about a wide operating frequency range but must sacrifice the upper limit for ideal power efficiency, capping it at 78.5% [12]. However, the class-R approach provides a wide load impedance design space for harmonic frequencies [13]–[15] and an ideal power efficiency of 100%, where the optimum power factor for the fundamental frequency is realized without affecting the optimized harmonic frequency load impedance. Thus, we have selected the class-R amplifier as the candidate for frequency selective design.

An example of a conventional band-selective class-R amplifier configuration consisting of transmission lines is shown in Fig. 1 (a). To obtain the highest efficiency, the treated harmonic number has to be increased as much as possible. However, since the circuit elements are increased for the harmonic treatment, insertion loss degrades the efficiency, especially for a higher operation frequency. On the other hand, it is well known that effective efficiency improvement is obtained by treating only the second harmonic. In addition, if the frequency difference between f_1 and f_2 is

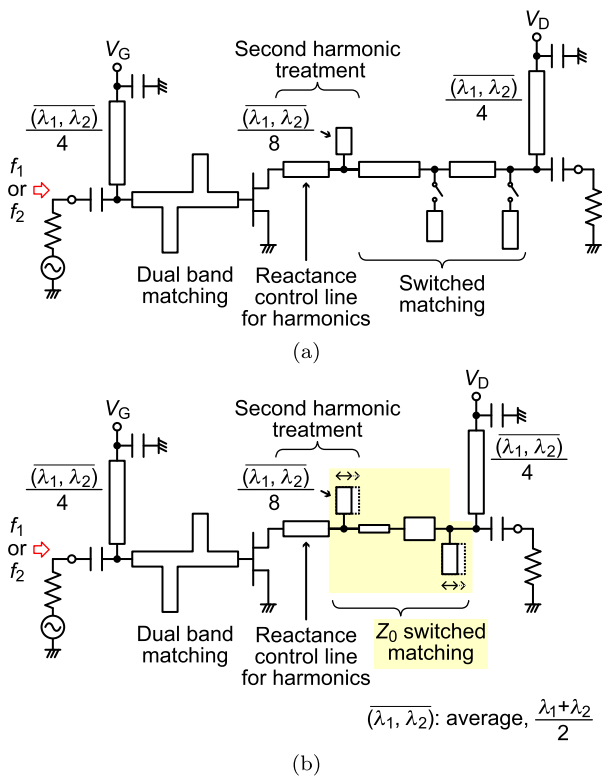

Fig. 1 (a) An example of a conventional band-selective class-R amplifier configuration consisting of transmission lines. (b) Proposed band-selective class-R amplifier configuration by changing the characteristic impedances.

Manuscript received February 15, 2018.
Manuscript revised May 30, 2018.

[†]The authors are with the Department of Communication Engineering and Informatics, University of Electro-Communications, Chofu-shi, 182–8585 Japan.
a) E-mail: k.mashimo@uec.ac.jp
b) E-mail: r.ishikawa@uec.ac.jp
c) E-mail: honjou@uec.ac.jp

DOI: 10.1587/transele.E101.C.751

about 10%, a common reactive termination circuit can be used for two second-harmonic treatments, since a reactance margin exists in the class-R design, as mentioned before. In this case, an average quarter-wavelength open-ended stub is used to make a short condition for the second harmonic, as shown in Fig. 1. Similarly, for drain- and gate-bias circuits, an average quarter-wavelength shortened stub is used, as shown in Fig. 1. In order to select the operation frequency, a load-matching circuit is switched for each fundamental frequency. In this case, two open-ended stubs are connected or disconnected by using switches to adjust the two optimum impedance values. For the input side, dual- or wide-band matching is applied.

Figure 1 (b) shows the proposed band-selective class-R amplifier configuration. The input matching and biasing are the same as those for the conventional one. For switching the load-matching circuit, the characteristic impedance of the average quarter-wavelength open-ended stub for the second harmonics is switched, in addition to that for the stub in a load-matching circuit, as shown in Fig. 1 (b). The characteristic impedance variation of the stub for the second harmonics does not affect the short condition for the harmonic treatment. When actual switching elements are used, insertion loss degrades the high-efficiency operation. In this case, the influence of the loss depends on where the switches are connected on the main line, owing to the different standing wave amplitude.

In this paper, the configurations in both Fig. 1 (a) and Fig. 1 (b) are investigated for a 4.5-/4.9-GHz band-selective GaN HEMT amplifier design. As a result, efficiency advantage was confirmed for the proposed configuration. The design procedure, including a comparison, and evaluation results for the proposed configuration are described.

2. Design of Band-Selective Amplifier

2.1 Load-/Source-Pull Simulation

In order to obtain a high-efficiency characteristic for each operation frequency on the class-R amplifier, optimum termination impedances at the fundamental frequencies and optimum termination reactance at the harmonic frequencies were estimated on a load-/source-pull simulation by using a circuit simulator (Keysight, ADS). The fundamental frequency was set to 4.5 and 4.9 GHz. Only the second harmonics were considered for both input and output sides. For the transistor, a 6-W-class GaN HEMT bare chip (CGHV1J006D, Cree) was assumed. For the simulation, a large-signal model provided from Cree was used.

Figure 2 shows the simulated impedance regions where a high-efficiency characteristic of more than 70% is maintained. The impedance regions are indicated as contour lines for the fundamental frequencies. For the second harmonics, the impedance regions are indicated on the periphery of the Smith chart, as the class-R design. In the load-/source-pull simulation, the impedance region for each target condition was estimated by fixing the other impedance conditions

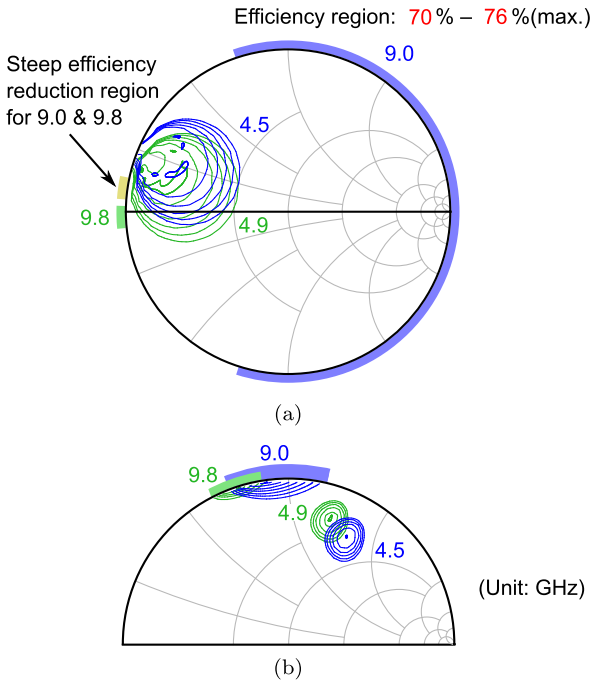

Fig. 2 Simulated impedance regions where a high-efficiency characteristic of more than 70% is maintained for (a) the source side and (b) the load side, estimated by a load-/source-pull simulation.

as optimum. Therefore, it is necessary to consider that the worst case will become less than 70% in the estimated regions.

In Fig. 2 (a), relatively wide impedance regions were obtained for the fundamental frequencies (4.5 and 4.9 GHz). On the other hand, for the second harmonics, the impedance region became narrow at 9.8 GHz, though it became wide at 9.0 GHz. A steep efficiency reduction region for both 9.0 and 9.8 GHz are also shown in Fig. 2 (a). From 62 to 50% efficiency drops were observed in this region. From these results, it is expected that the input matching circuit can be constructed with fixed wide-band matching between 4.5 and 4.9 GHz, though the steep efficiency reduction region at 9.0 and 9.8 GHz has to be excluded.

In Fig. 2 (b), the impedance regions were relatively narrow at 4.5, 4.9, 9.0, and 9.8 GHz. However, the variation of the efficiency outside the regions is different for each frequency. A large efficiency reduction was observed outside the regions for the fundamental frequencies. On the other hand, the efficiency reduction was not so large in case of an actual design for the second harmonic frequencies. The impedance regions inside of the Smith chert for the second harmonics are also shown in Fig. 2 (b). When the impedance for 9.8 GHz was shifted to the 9.0 GHz region, more than 62% was maintained. If the average quarter wavelength open-ended stub is used for shunting the second harmonics, the impedance moves to clockwise direction on the periphery of the Smith chert in the high-efficiency region even if perfect reflection conditions cannot be maintained for them. For the fundamental frequencies, the optimum impedance moves gently in a counterclockwise direction on the Smith

chart in accordance with the frequency increase, like a decrease in parallel capacitance. Therefore, it is expected that only the characteristic impedance of the second harmonic shunt stub will be changed for the switching of the proposed configuration.

2.2 Characteristic Impedance Switching by a Parallel Additional Line

By adding a parallel additional line to an open-ended stub in parallel, an equivalent characteristic impedance is changed, like a parallel connection. Simulated reactances by using an electromagnetic (EM) simulator (ADS Momentum) for three connection conditions are shown in Fig. 3. An electrical length of the open-ended stub and the additional line was set to the average quarter wavelength of 9.0 and 9.8 GHz. In addition, the line widths were set to 0.9 and 2 mm for the open-ended stub and the additional line, respectively.

When the open-ended stub and additional line were not connected, as shown in Fig. 3 (a), the stub impedance was higher than that for the other conditions, since there was no parallel component. When the open-ended stub and the additional line were connected at only the stub port, as shown in Fig. 3 (b), the stub reactance was effectively changed as a capacitance variation at the fundamental frequency region. However, a resonance appeared at the second frequency region. This is attributed to a slight electrical length difference between the open stub and the additional line. As a result, it is difficult for only a parallel connection of stubs to control the correct electrical lengths. When the open-ended stub and the additional line were connected at both sides of the stub, as shown in Fig. 3 (c), the same reactance variation at the fundamental frequency region was obtained as with the parallel connection shown in Fig. 3 (b). Additionally, the resonance that appeared in the parallel connection was removed. This is attributed to the averaging of the electrical lengths between the stub and the line. Moreover, the short condition around the second harmonic frequency was shifted between connected and non-connected conditions, owing to a dispersion characteristic of the lines. This was convenient when the connected condition was assigned to the lower operation frequency, i.e., 4.5 GHz.

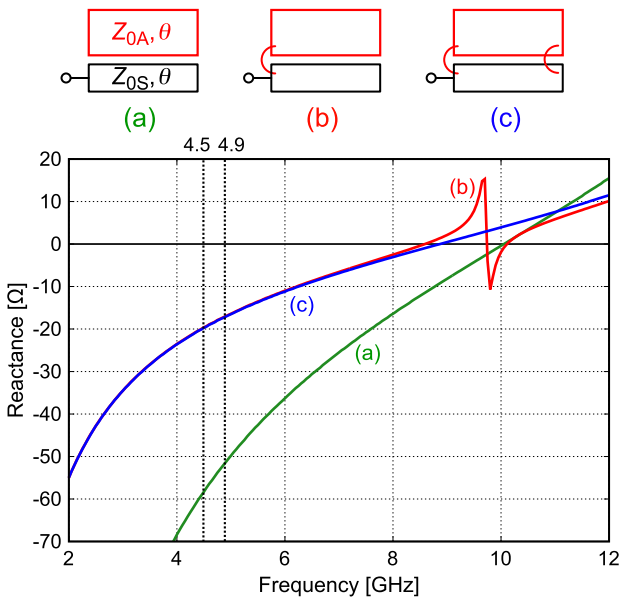

Fig. 3 Frequency dependence of electromagnetic (EM) simulated reactance for the following conditions: (a) no connection, (b) connected at only the stub port, and (c) connected at both sides of the stub.

The stub reactance X at the fundamental frequency is represented as follows:

$$X = \begin{cases} -\frac{Z_{0S}Z_{0A}}{Z_{0S}+Z_{0A}}\cot\theta \simeq -\frac{Z_{0S}Z_{0A}}{Z_{0S}+Z_{0A}} & @\text{connected} \\ -Z_{0S}\cot\theta \simeq -Z_{0S} & @\text{non-connected}, \end{cases} \quad (1)$$

where, Z_{0S} and Z_{0A} are the characteristic impedances of the open stub and the additional line, respectively. θ is the electrical length and $\theta \simeq \pi/4$ is fulfilled, since θ is close to $\pi/2$ at the second harmonic frequencies. From this result, it works as a switchable capacitance.

2.3 Amplifier Operation for Switching Conditions

By using characteristic impedance switching, the 4.5-/4.9-GHz band-selective GaN HEMT amplifier was designed. From the load-/source-pull simulation result described in Sect. 2.1, only the characteristic impedance of the average quarter-wavelength open-ended stub for shunting the second harmonics was switched for the design. First, the matching circuit at 4.9 GHz was adjusted by setting the switched stub to the "non-connected" condition with a low capacitance. Then, the matching circuit at 4.5 GHz was adjusted by setting the switched stub to the "connected" condition with a high capacitance.

Figure 4 shows the designed load circuit. For comparison, a load-circuit design based on the conventional configuration is also shown. For the conventional configuration using a GaN HEMT, two switched stubs are used to obtain a sufficient frequency difference.

Figure 5 shows the simulated frequency dependences of the efficiency characteristics. In the simulation, two cases were assumed: 1) that an ideal switch was used and 2) that the switch was assumed to be a 2-Ω resistor in the on-state and a 0.1-pF capacitor in the off-state, as an actual condition mentioned in Sect. 5. From Fig. 5, high-efficiency and frequency-selective characteristics were obtained for both configurations when the ideal switch was used. However, in the actual switching condition, a large efficiency reduction was observed for the conventional configuration due to an insertion loss. It was confirmed that the influence of the loss for the proposed configuration was smaller than that for the conventional one, in this case. In the on-state, where the loss of the series parasitic resistance is affected, the maximum efficiency decreases by about 4% in the proposed method, and the maximum efficiency decreases by about 11% in the conventional method. Therefore, the band-selective amplifier based on the proposed configuration was fabricated and evaluated.

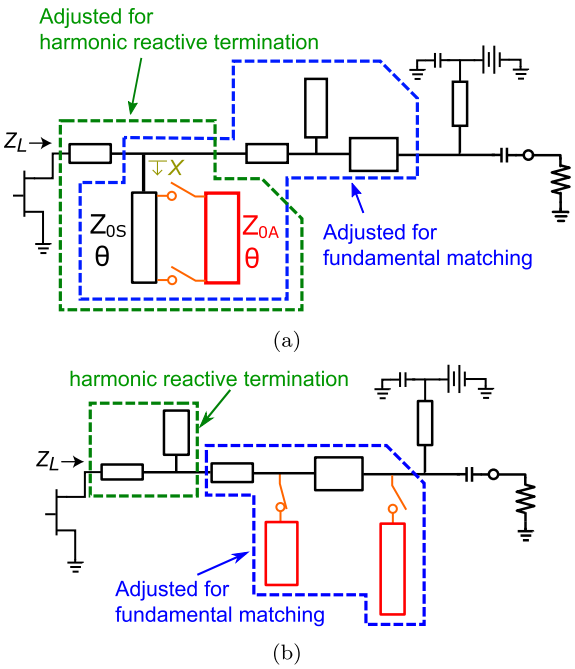

Fig. 4 Designed load circuits for GaN HEMT based on (a) the proposed circuit configuration and (b) the conventional one.

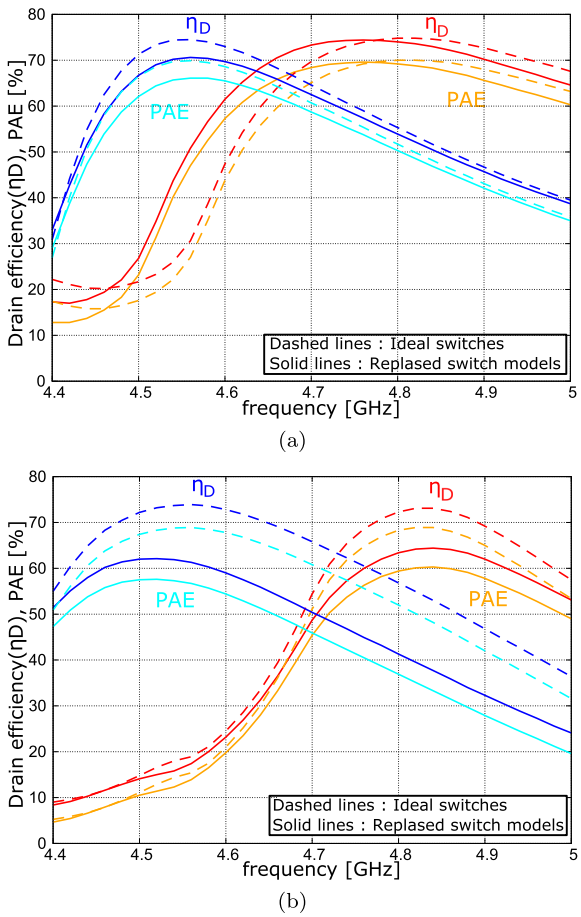

Fig. 5 Simulated frequency dependences of efficiency characteristics for (a) the proposed configuration and (b) the conventional configuration. Both ideal and actual switches are assumed for the simulation as a comparison.

3. Fabrication of the Proposed Band-Selective Amplifier

From the load-/source-pull simulation results shown in Fig. 2, input- and output-matching circuits were fabricated. Figure 6 shows the fabricated 4.5-/4.9-GHz band-selective GaN HEMT amplifier. For the input- and output-matching circuits, resin substrates (Megtron7, $\varepsilon_r = 3.4$, $\tan\delta = 0.002$, Panasonic) with a thickness of 0.4 mm were used.

Figure 7 shows EM-simulated and measured source and load impedances. The target regions shown in Fig. 2 to obtain a high-efficiency characteristic are also shown. In the measurement, the connected and non-connected conditions

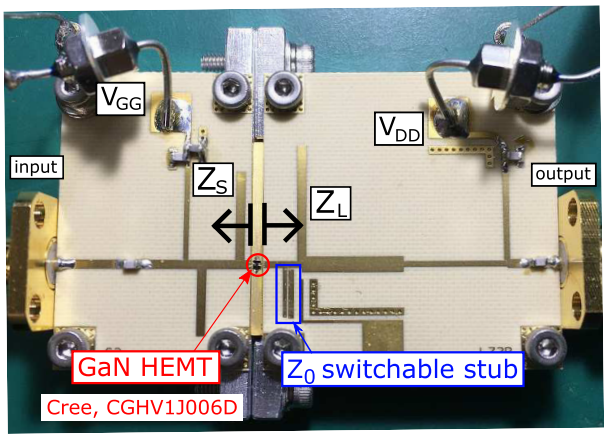

Fig. 6 Fabricated 4.5-/4.9-GHz band-selective GaN HEMT amplifier.

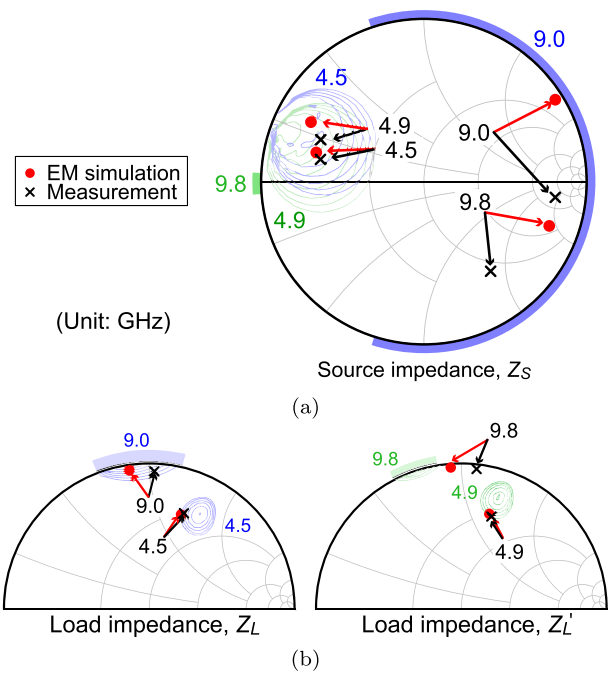

Fig. 7 EM-simulated and measured (a) source and (b) load impedance. Target regions shown in Fig. 2 to obtain a high-efficiency characteristic are also shown.

were realized with and without Au bonding wires, respectively, for ease of evaluation. From Fig. 7 (a), the measured source impedances at the fundamental frequencies were included in each target region, as well as in the simulated ones. In addition, the measured source impedances at the second harmonic frequency of 9.0 GHz was also close to the target region, though those gently deviated from the simulated ones, owing to a substrate permittivity deviation at the higher frequency. Furthermore, those was gently apart from the periphery of the Smith chart, owing to loss. For 9.8 GHz, both the measured and simulated impedances were not close to the target region. However, this did not induce a large efficiency reduction.

From Fig. 7 (b), the measured and simulated load impedances at the fundamental frequencies for each switched condition were almost the same and are included in each target region. For 9.0 GHz, those were also included in each target region, though those at 9.8 GHz gently deviated from the target region.

4. Confirmation of Band Selectivity by Using Bonding Wires

To confirm the band selectivity for the proposed amplifier configuration, Au bonding wires were used for the connected condition, instead of an actual switch element. The frequency dependences of the maximum drain efficiency ($\eta_{D\max}$), maximum power-added efficiency (PAE_{max}), saturated output power (P_{sat}), and gain for the connected and non-connected conditions are shown in Fig. 8. The drain and gate bias voltages were set to 40 V and −2.7 V, respectively. From Fig. 8, it was confirmed that the band could be switched to obtain a high-efficiency characteristic. The differences in peak frequencies were due to a slight impedance mismatching. The input-output power response, gain, and efficiency characteristics at 4.66 GHz for the connected condition and at 4.92 GHz for the non-connected condition are shown in Fig. 9. A $\eta_{D\max}$ of 66% and 70% and a PAE_{max} of 62% and 66% were obtained at 4.66 and 4.92 GHz, respectively, with a P_{sat} of 38 dBm.

5. Evaluation of the Proposed Band-Selective Amplifier with PIN Diodes

5.1 Efficiency Performances

To electrically select the operation band, a PIN diode was used as a switch, as shown in Fig. 10. Since a GaN HEMT amplifier operates with a high-voltage DC power supply, a high-breakdown-voltage characteristic is required. In addition, a low series resistance in the on-state and a low capacitance in the off-state are also required for low insertion loss and high-frequency operation, respectively.

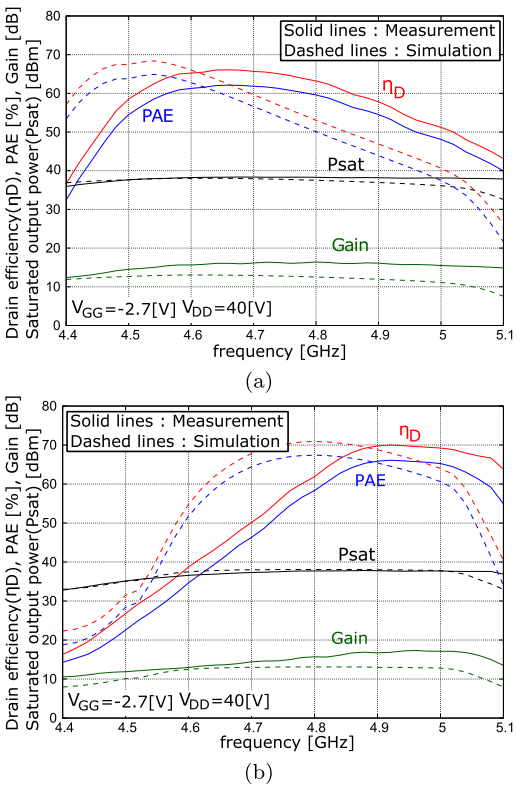

Fig. 8 Frequency dependences of maximum drain efficiency ($\eta_{D\max}$), maximum power-added efficiency (PAE_{max}), saturated output power (P_{sat}), and gain for (a) the connected and (b) non-connected conditions, by using bonding wires.

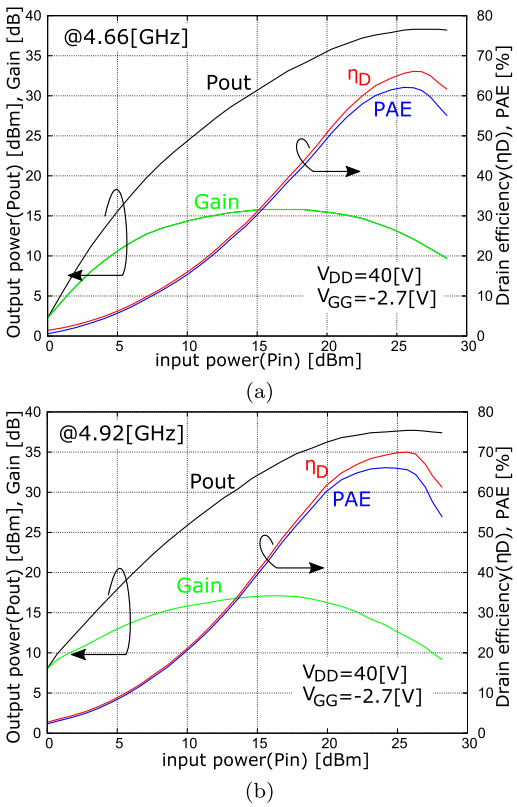

Fig. 9 Input-output power response, gain, and efficiency characteristics (a) at 4.66 GHz for the connected condition and (b) at 4.92 GHz for the non-connected condition.

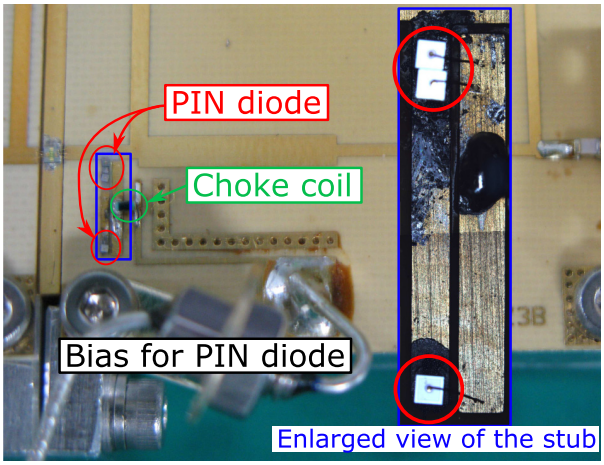

Fig. 10 Mounted PIN diodes for the fabricated 4.5-/4.9-GHz band-selective GaN HEMT amplifier.

In this research, PIN diodes (MA4P161-134, Resistance: 1.5 Ω, [@500 MHz, 10 mA] Total Capacitance: 0.1 pF [V_r = −15 V], MACOM) were used. In addition, in order to reduce the resistance, three diodes connected in parallel were used at the stub port side. A DC bias voltage for the PIN diodes was supplied via a choke coil (33 nH, LQW15 series, Murata) by stacking the drain DC bias voltage for the GaN HEMT.

The frequency dependences of $\eta_{D\max}$, $\mathrm{PAE}_{\max}$, $\mathrm{P}_{\mathrm{sat}}$, and the gain for the on/off conditions by switching the PIN diodes are shown in Fig. 11. Those for the measured characteristic shown in Fig. 8 are also shown for comparison. From Fig. 11 (a), the efficiency peak is reduced due to the resistance of the PIN diodes, though the reduction was within about 4%. From Fig. 11 (b), the efficiency peak is shifted due to the capacitance of the PIN diodes, though there was no efficiency reduction. The fabricated GaN HEMT amplifier exhibited a $\mathrm{PAE}_{\max}$ of 57% and 66%, a $\eta_{D\max}$ of 62% and 70%, and a $\mathrm{P}_{\mathrm{sat}}$ of 38 dBm at 4.6 and 5.0 GHz, respectively, for each switching condition.

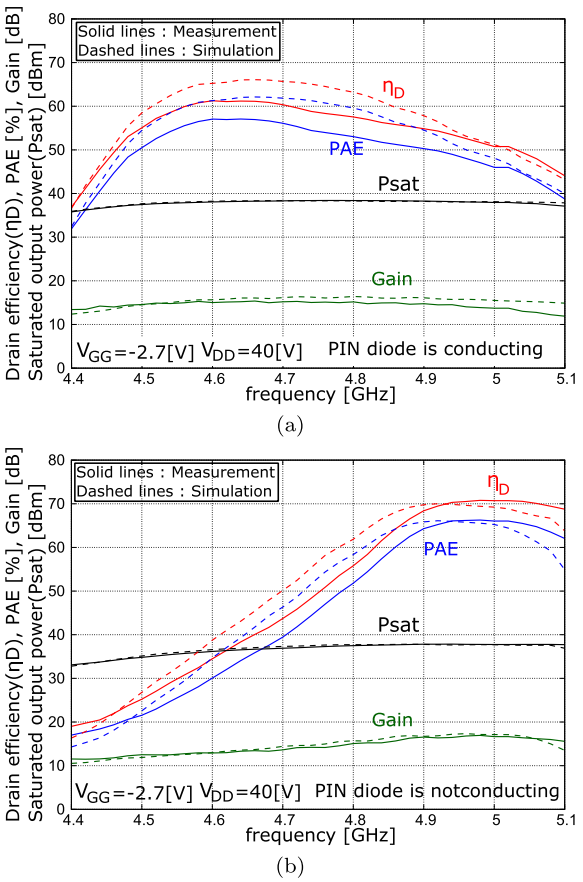

Fig. 11 Frequency dependences of $\eta_{D\max}$, $\mathrm{PAE}_{\max}$, $\mathrm{P}_{\mathrm{sat}}$, and gain for (a) connected and (b) non-connected conditions, by using PIN diodes.

5.2 Distortion Evaluation

Since the switching element is a nonlinear device, the linearity of the amplifier had to be confirmed. Then, a digital modulated signal was applied to the fabricated amplifier. For the evaluation, a 256 quadrature amplitude modulation (QAM) signal with a symbol rate of 10 Msps and a peak-to-average power ratio (PAPR) of 6.32 dB provided by a signal generator (N5172B, Keysight) was inputted to the fabricated amplifier, and the output signal was analyzed by a signal analyzer (MSOS804A, Keysight) to estimate the error vector magnitude (EVM).

The output spectra for each condition are shown in Fig. 12 (a). In the measurement, the center frequencies were set to 4.6 and 5.0 GHz at the connected and non-connected conditions, respectively. In addition, the average input power was set to 15 dBm, corresponding to the 7-dB out-

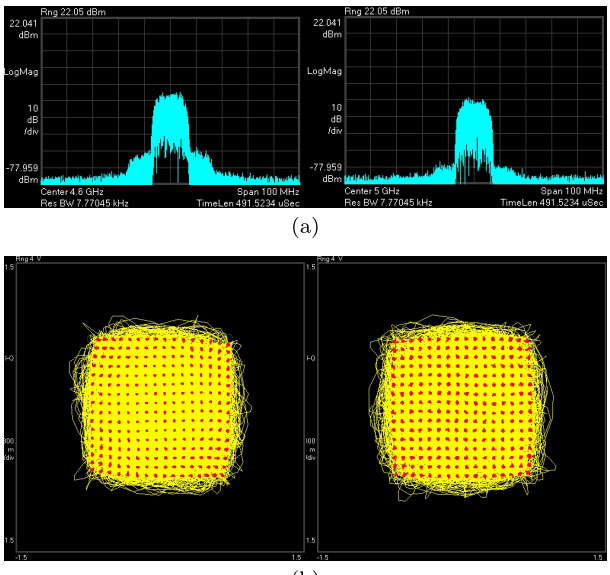

Fig. 12 (a) Measured output spectra and (b) constellation for 256 QAM signal with a symbol rate of 10 Msps with an input power of 15 dBm. Each figure on the left shows the connected condition (4.6 GHz) and each figure on the right shows the non-connected condition (5.0 GHz).

put back-off condition. From Fig. 12 (a), the adjacent channel leakage power ratio (ACLR) was about 35 and 40 dBc for the connected and non-connected conditions, respectively. These values are better than those when using a bonding wire (about 32 and 28 dBc for the connected and non-connected conditions). In the case of using a bonding wire, since the signal of 256 QAM could not be discriminated, it was measured using a signal of 64 QAM. Since the output power for each condition differed from the others due to the gain difference (16.7 dB at 4.6 GHz and 14.8 dB at 5.0 GHz), each ACLR was also different. Figure 12 (b) shows the measured constellations. The measured EVM was 1.6% and 1.3% for the connected and non-connected conditions, respectively. From these results, it was confirmed that a particular linearity degradation was not observed for the use of PIN diodes.

6. Conclusion

A harmonic reactive termination type band-selective high-efficiency GaN HEMT amplifier that involves switching the effective characteristic impedance was developed. By using PIN diodes as switches for the proposed configuration, the operation frequency to obtain a high-efficiency characteristic could be switched with a reduced influence of diode insertion loss. The fabricated 4.5-/4.9-GHz band-selective GaN HEMT amplifier exhibited a maximum power-added efficiency of 57% and 66%, a maximum drain efficiency of 62% and 70%, and a saturation output power of 38 dBm at 4.6 and 5.0 GHz, respectively, for each switching condition. In addition, for a 256 QAM signal input, it was confirmed that a particular linearity degradation was not observed with the use of PIN diodes.

Acknowledgements

This work was partly supported by the Ministry of Internal Affairs and Communications.

References

[1] N.O. Sokal and A.D. Sokal, "Class-E – A new class of high efficiency tuned single-ended switching power amplifiers," IEEE J. Solid-State Circuits, vol.SC-10, pp.168–176, June 1975.
[2] F.H. Raab, "Class-F power amplifiers with maximally flat waveforms," IEEE Trans. Microw. Theory Techn., vol.45, no.11, pp.2007–2012, Nov. 1997.
[3] S.C. Cripps, RF Power Amplifiers for Wireless Communications, 2nd ed., Artech House, Norwood, MA, 2006.
[4] S.H. Ji, C.S. Cho, J.W. Lee, and J. Kim, "Concurrent dual-band class-E power amplifier using composite right/left-handed transmission line," IEEE Trans. Microw. Theory Techn., vol.55, no.6, pp.1341–1347, June 2007.
[5] R. Negra, A. Sadeve, S. Bensmida, and F.M. Ghannouchi, "Concurrent dual-band class-F load coupling network for applications at 1.7 and 2.14 GHz," IEEE Trans. Circuits Syst. II, Exp. Briefs, vol.55, no.3, pp.259–263, March 2008.
[6] Y. Jeong, G. Chaudhary, and J. Lim, "A dual band high efficiency class-F GaN power amplifier using a novel harmonic-rejection load network," IEICE Trans. Electron., vol.E95-C, no.11, pp.1783–1789, Nov. 2012.
[7] J. Enomoto, R. Ishikawa, and K. Honjo, "A 2.1/2.6 GHz dual-band high-efficiency GaN HEMT amplifier with harmonic reactive terminations," Proc. 2014 European Microw. Conf., Rome, Italy, pp.1488–1491, Oct. 2014.
[8] M. Kamiyama, R. Ishikawa, and K. Honjo, "5.65 GHz high-efficiency GaN HEMT power amplifier with harmonic treatment up to fourth order," IEEE Microw. Wireless Compon. Lett., vol.22, no.6, pp.315–317, June 2012.
[9] F.H. Raab, "Electronically tunable class-E power amplifier," IEEE MTT-S Int. Microwave Symp. Digest, pp.1513–1516, May 2001.
[10] L. Larcher, R. Brama, M. Ganzerli, J. Iannacci, B. Margesin, M. Bedani, and A. Gnudi, "A MEMS reconfigurable quad-band Class-E power amplifier for GSM standard," IEEE 22nd Int. Conference on Micro Electro Mechanical Systems (MEMS '09), Australia, pp.864–867, 2009.
[11] G. Nikandish, E. Babakrpur, and A. Medi, "A harmonic termination technique for single- and multi-band high-efficiency class-F MMIC power amplifiers," IEEE Trans. Microw. Theory Techn., vol.62, no.5, pp.1212–1220, 2014.
[12] N. Tuffy, A. Zhu, and T.J. Brazil, "Class-J RF power amplifier with wideband harmonic suppression," IEEE MTT-S Int. Microwave Symp. Digest, June 2011. DOI: 10.1109/MWSYM.2011.5972873.
[13] J. Enomoto, R. Ishikawa, and K. Honjo, "Second harmonic treatment technique for bandwidth enhancement of GaN HEMT amplifier with harmonic reactive terminations," IEEE Trans. Microw. Theory Techn., vol.65, no.12, pp.4947–4952, Dec. 2017.
[14] Y. Takagi, R. Ishikawa, and K. Honjo, "Wide-band high-efficiency GaN HEMT amplifier based on dual-band multi-harmonic treatments," 2017 47th European Microwave Conference (EuMC), pp.468–471, 2017.
[15] K. Mashimo, R. Ishikawa, and K. Honjo, "4.5-/4.9-GHz-band tunable high-efficiency GaN HEMT power amplifier," 2017 47th European Microwave Conference (EuMC), pp.460–463, 2017.

Kazuki Mashimo received the B.E. degree in information and communication engineering from the University of Electro-Communications, Tokyo, Japan, in 2017, and is currently working toward the M.E. degree at the University of Electro-Communications, Tokyo, Japan.

Ryo Ishikawa received the B.E., M.E., and D.E. degrees in electronic engineering from Tohoku University, Sendai, Japan, in 1996, 1998, and 2001, respectively. In 2001, he joined the Research Institute of Electrical Communication, Tohoku University, Sendai, Japan. In 2003, he joined the University of Electro-Communications, Tokyo, Japan. His research interest is the development of microwave compound semiconductor devices and related techniques. Dr. Ishikawa is a member of the Japan Society of Applied Physics. He was the recipient of the 1999 Young Scientist Award for the Presentation of an Excellent Paper of the Tohoku Chapter, Japan Society of Applied Physics.

Kazuhiko Honjo received the B.E. degree from the University of Electro-Communications, Tokyo, in 1974, and the M.E. and D.E. degrees in electronic engineering from the Tokyo Institute of Technology, Tokyo, in 1976 and 1983, respectively. From 1976 to 2001, he worked for NEC Corporation, Kawasaki, Japan. In 2001, he joined the University of Electro-Communications as a professor in the Information and Communication Engineering Department. He has been involved in research and development of high-power/broadband/low-distortion microwave amplifiers, MMICs, HBT device and processing technology, miniature broadband microwave antennas and FDTD electro-magnetic wave and device coanalysis. Prof. Honjo received both the 1983 Microwave Prize and the 1988 Microwave Prize granted by the IEEE Microwave Theory and Techniques Society. He also received the 1980 Young Engineer Award, and the 1999 Electronics Award both presented by the Institute of Electrical, Information and Communication Engineers (IEICE), Japan. He is Fellow of IEEE.